Progress In Electromagnetics Research C, Vol. 62, 61–70, 2016

Compact Rectenna Design for Lossy Paper Substrate at 2.45 GHz

Ines Kharrat[1, *], Pascal Xavier[1], Tan-Phu Vuong[1], and Guy Eymin Petot Tourtollet[2]

Abstract—This work presents a compact rectenna based on printed on paper electronics. The rectenna is printed using mass production technique on an environmental-friendly and flexible paper substrate. Only one ink layer is used. The characterized paper substrates present minimum tangent losses of 0.08. It shows at most 40 times higher tangent loss than commercial substrates (Rogers Ultralam2000). A reduction of 50% of dielectric losses can be achieved by a good selection of the paper type; the selected paper substrate is a corrugated cardboard with 0.04 loss tangent value. The designed rectenna is based on two series-mounted SMS7630 Schottky diodes. Co-design technique has been used in order to integrate different blocks for additional loss reduction. The goal of our work is the use of a recyclable cardboard substrate with low-losses compared to classical paper substrate and high losses compared to commercial substrates. The printed on cardboard rectenna presents similar performances to a rectenna etched on commercial substrates. This device aims to convert high voltage levels (1 V) at low power levels (−15 dBm) for self-sustainable devices. For our application, an electrochromic display is supplied for anti-counterfeiting purposes. When a smartphone operating on Wi-Fi mode is close, the printed rectenna exhibits 970 mV DC which is sufficient to turn on the electrochromic display.

1. INTRODUCTION

Printed, organic or flexible electronics are very active and connected research fields [1]. Flexible electronics allows the design on a flexible and environment-friendly substrate which offers a wide range of new applications. In printed electronics, manufacturing technique costs are much lower than those of the silicon industry, which is why even if the performances between a silicon chip and an organic transistor cannot be compared, the cost/performance ratio makes organic option very interesting.

Another progress concerns the development of Internet of Things. It has become increasingly common to use sensors in many areas (space, military, medical, domestic), especially in dangerous or limited access places. The conventional battery power has limited autonomy, requires periodic replacement and is expensive to recycle. Wireless transfer energy is a technique to harvest energy. Since the first experience of electromagnetic wave propagation realized by Heinrich Hertz in 1888 [2], followed by the experiments of Nicola Tesla in 1899, point to point transmission energy has become a tremendous research topic.

Merge the two technologies can lead to new applications and new features to the paper as well as facilitate the integration of rectennas in the systems when using flexible substrates.

Diverse energy harvesting circuit topologies have recently been developed. They are generally based on the nonlinear characteristics of diodes that allow the AC to DC energy conversion. These topologies depend on different criteria including diode position and antenna design: single series structure [3], shunted mounted diode structure [4, 5] or voltage doubler structure [6] which allows reaching higher DC voltage. Several kinds of antennas have been used for harvesting energy circuits such as patch

Received 30 September 2015, Accepted 27 January 2016, Scheduled 12 February 2016

* Corresponding author: Ines Kharrat (ineskharrati@gmail.com).

[1] Université Grenoble-Alpes, IMEP-LAHC, 3 Parvis Louis Néel, CS 50257-38016 Grenoble, France. [2] Centre Technique du Paper, Domaine Universitaire, BP 251, 38044 Grenoble, France.

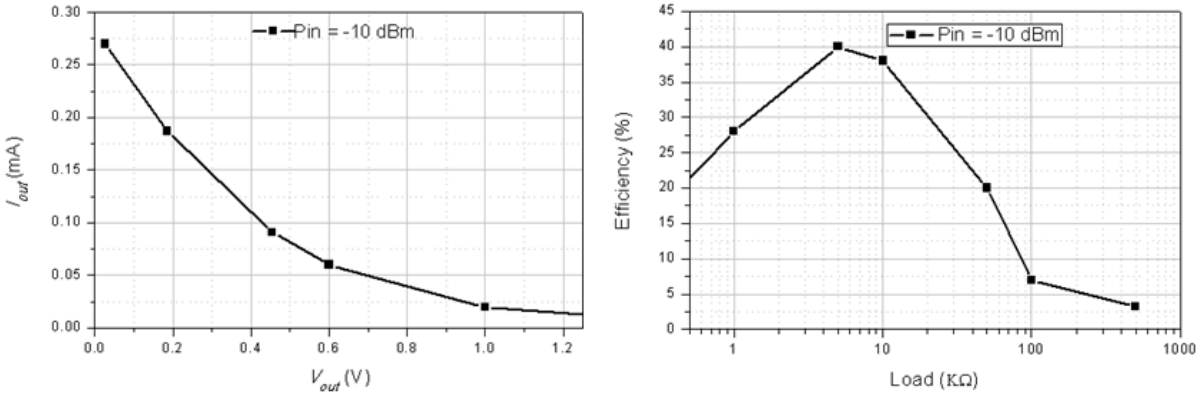

Figure 1. Simulated series-mounted rectenna characteristics: (a) current-voltage, (b) efficiency-output load.

antenna [7], dipole antenna [8], multilayer antenna [9] and antenna array [10]. Designers are often faced to a choice of a figure of merit: either high output voltage or high conversion efficiency which is defined as the ratio between DC power at the load and the RF power at the receiving antenna input. In [11], it has been demonstrated that this choice depends on the output load value. Figure 1 shows the efficiency and output voltage for a typical series-mounted rectenna. We can deduce that the efficiency of the rectenna is optimal for a given load value, which in this case is around 5 kΩ while high output voltage needs high load values.

In this paper, the load is fixed. It corresponds to an electrochromic planar display [12], an intelligent display, which is connected to the rectenna in order to check a product authenticity. Protection against counterfeiting represents the intended application. A code should appear when approaching a smartphone working on the Wi-Fi band. Electrochromism technology consists in the change of color for some materials in a reversible manner. Various materials can be used to construct electrochromic devices. These materials differ from each other based on the required voltage, contrast and speed change [13]. The display is similar to a battery, its charging time must be very fast and its discharge time slow. These characteristics depend on the display impedance which should be as high as possible. The equivalent impedance is equal to 30 kΩ. For a given power, an electrochromic display requires DC voltage as high as possible, so the efficiency might not be optimal.

The intended application requires the energy harvesting circuit to be designed on low-loss paper, a low cost recycling material, and for low input power (typically −15 dBm).

The first part of this paper describes how the rectenna recovers power and converts it. In the next part, a study of different paper substrates is developed and a low loss paper is selected. Then, the rectenna miniaturization method using co-design is described. Finally, the simulated and measured circuit behavior is presented.

2. PAPER SUBSTRATE CHOICE

2.1. Classical Paper Characterization

Paper substrate is an unusual material for electronics in terms of losses and mechanical properties. Therefore, for simulating the circuit performances, a preliminary step of dielectric characterization is needed. In the domain of planar circuits and transmission lines, there are many characterization methods, but the implementation of these methods for a flexible and copper-free substrate is complex and leads to significant measurement uncertainties [14]. The resonant cavity method has been demonstrated to have the best accuracy for thin substrate, e.g., paper substrate [15].

However, this method can be performed only in some frequencies which correspond to the resonant frequencies of the cavity. Therefore, transmission line method was used as a complementary method.

This method allows to ensure that the permittivity is not dispersive in the band of interest (0.5 GHz to 4 GHz). This second method is chosen because it is easy to implement and works over a wide frequency range.

Table 1 summarizes the complex permittivity results for classic paper samples, for example bond paper, cardboard, photo paper. The different paper samples, $SP1$ to $SP4$, are classical papers that differ in their manufacturing process and/or surface finishing. Their dielectric constant values are highly specific to the paper substrate. The measurement uncertainty is mainly due to the sample width measurement [16]. These uncertainties were evaluated and presented in Table 1. It can be noticed that the dielectric losses are high. Investigations were made to find the source of the losses in order to minimize them. Moisture tests were performed by placing water drops on the substrate: the results show that this type of paper is insensitive to humidity. The sources of losses are intrinsic. It depends on the characteristics of the cellulose [17]. Ro-Ultralam 2000 substrate (an Epoxy based substrate) characteristics have been presented in Table 1 in order to compare its characteristics with the paper. Its losses are 35 times lower than paper losses.

Table 1. Classical paper characterization results.

Substrate	$SP1$	$SP2$	$SP3$	$SP4$	Rogers Ultralam 2000
Thickness (mm)	0.18	0.56	0.365	0.56	0.37
Density (Kg/m^3)	1015	610	572	619	
$\varepsilon_r \pm 0.003$	2.95	2.48	2.47	2.56	2.5
$\tan\delta \pm 5.10^{-4}$	0.083	0.11	0.081	0.1	0.0019

2.2. Low-Loss Paper Substrate: Corrugated Cardboard

To deal with dielectric loss problem, corrugated cardboard was chosen as a substrate. Thanks to its corrugation, an extra air layer (loss free) fills the void, instead of getting a homogeneous paper layer with high losses. Figure 2(b) describes the corrugated cardboard and compares with classic paper (Figure 2(a)).

Different corrugated cardboards (substrates) with different air thicknesses (H) have been characterized. Table 2 presents four types of corrugated cardboards ($C1$ to $C4$). It shows the relationship between the air thickness in the corrugated cardboard and dielectric characteristics. If air thickness increases, dielectric loss value decreases.

With a tangent loss of 0.042, the cardboard '$C4$' was chosen since the tangent loss value is divided by 2 compared to conventional paper substrate.

Despite the good characteristic of the corrugated cardboard, dielectric losses still have an impact on the overall circuit performances compared to conventional substrates. In order to improve the performances of the rectenna and reduce its size, a "co-design" seems to be a promising solution.

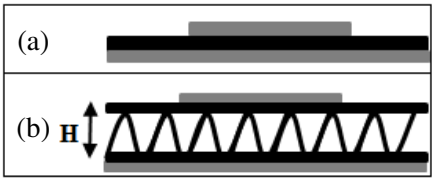

Figure 2. Layout of (a) classic paper, (b) corrugated cardboard.

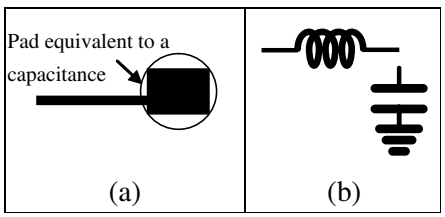

Figure 3. (a) Layout of the end of DC filter, (b) equivalent circuit of DC filter.

Table 2. Comparison between different cardboard substrates.

Cardboard	$C1$	$C2$	$C3$	$C4$
Thickness (H) (mm)	0.787	1.48	1.58	3
ε_r	2.14	1.55	1.52	1.41
$\tan\delta$	0.068	0.054	0.047	0.042

3. MINIATURIZED RECTENNA DESIGN

The basic six subsystems for rectenna design are: antenna, RF-side low pass filter, impedance matching network, one or more diodes, DC-side low pass filter, and load. The antenna collects energy from the EM sources. The rectifier consists of one or more Schottky diodes. The diode has nonlinear behavior and therefore generates high harmonic signals for each fundamental frequency collected on either side of the diode. For this reason, two low-pass filters (RF side and DC side) are designed on each side of the rectifier circuit. The RF side filter aims to avoid energy losses by eliminating the harmonic radiation of higher order modes which are reflected back to the antenna. The DC side filter allows the DC current to flow to the load and block all RF components including the fundamental component (2.45 GHz). An impedance matching network is added between the RF filter and the diode to ensure good matching for maximum power transfer. In this work, the "co-design" technique is used in order to make the system more compact. The design flow is explained in the following. Optimization process begins from the load to the antenna. The load, in our case, is a printed on paper electrochromic display whose impedance is 30 kΩ at high frequencies with zero bias. First step consists of optimizing the DC side filter. Then the diode choice is justified. Finally, the low-pass RF-side filter is integrated in the design of the antenna.

3.1. Low-Pass DC-Side Filter

The role of the DC filter consists of smoothing the DC current and voltage while rejecting the fundamental frequency and high frequency harmonics. In the bibliography, radial stubs or localized capacitances are widely used [18, 19].

In order to connect the display to the circuit, two 15 mm × 7 mm square pads were etched at the end of the circuit (Figure 3(a)). Each pad corresponds to a capacitance at high frequencies, associated to a transmission line that connects the diode to the pads. The transmission line presents a high impedance. Both pads and high impedance lines form a low-pass filter (inductance + capacitance) as shown in Figure 3(b). The values of capacitance and inductance were calculated from the dimensions of the lines. With 13.5 nH and 0.44 pF, the resulting cut-off frequency of the low-pass filter is equal to 2.065 GHz. Therefore, the DC filter (stubs or capacitances) can be removed. The dimensions of the line connecting the diode to the square pad require optimization to allow better filtering abilities.

3.2. Schottky Diode

The choice of the diode is very crucial since its characteristics have a direct impact on the rectenna performance. This choice depends on many factors: operating frequency band, power level, and its Spice parameters. SMS 7630-093 [20], a zero bias diode, presents an extremely low barrier height and is suitable for 2.45 GHz. The equivalent circuit of a Schottky diode consists of a series resistance R_S which limits the efficiency, a junction capacitance C_j which affects how harmonic currents oscillate through the diode in parallel and a junction resistance R_j which depends on the total current flowing through the device. Low values of C_j, R_S and R_j are desired. Compared to other diodes such as HSMS2850 or HSMS2860, the selected diode presents better performances.

3.3. Antenna and Harmonic Rejection Filter Co-Design

In order to make the rectenna more compact, the co-design technique is used. In our case, it consists in integrating the low-pass RF side filter into the antenna in order to reject high harmonics generated

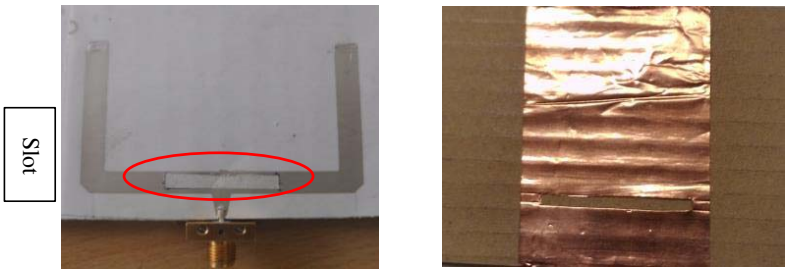

Figure 4. Photograph of the fabricated double monopole antenna, (a) front side, (b) back side.

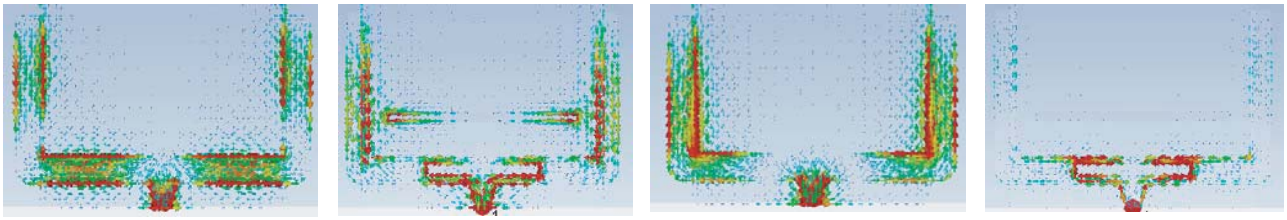

Figure 5. Simulated surface current distribution of the double monopole antenna, (a) without slot at 2.45 GHz, (b) with slot at 2.45 GHz, (c) without slot at 4.9 GHz and (d) with slot at 4.9 GHz.

by the diode. In addition, by reducing the size and number of distributed technology elements, the conductive losses will be reduced and therefore lead to better performances. In our case, the RF filter is integrated in the receiving antenna. A photograph of the $\lambda/2$ double monopole antenna is presented in Figure 4. The antenna dimensions are 60 mm $\times$ 30 mm. The dielectric used in Figure 4 is the corrugated cardboard "*C*4" with a height of 3 mm, permittivity of 1.41 and dielectric losses of 0.042. The antenna is printed in a single layer of silver-based ink. The ground plane (Figure 4(b)) is made with a copper tape. The slot is made in the ground plane in order to improve the impedance matching at 2.45 GHz. The resulting antenna has a main resonant frequency at 2.45 GHz. The slot on the upper side of the antenna was inserted in order to eliminate the resonance at 4.9 GHz, which corresponds to the first higher harmonic. The surface current distribution in the antenna with and without slot is depicted in Figure 5. It shows that at 2.45 GHz the current distribution is not affected when inserting the slot. However, at 4.9 GHz current lines are suppressed. The measured reflection coefficient is equal to -18 dB at 2.45 GHz (Figure 6(a)) ensuring a filtering for the three higher harmonics. The measured and simulated antenna gains are described in Figure 6(b)). It shows a level of 4 dBi of gain.

The proposed final diagram of the rectifier is described in Figure 7(a). The dimensions of the new rectifier are reduced by 30% compared to classical rectifer [21].

4. SIMULATION RESULTS

The rectifier is composed of two SMS7630 diodes and a display whose resistance is equal to 30 kΩ. Two diodes have been used to maximize the output voltage of the circuit. The diodes are connected in opposite ways, for a full-wave rectifying effect. The lines connecting the diodes to the square pad and to the input set up the matching between parts of the circuit. Figure 7(a) shows the rectifier pattern as well as the dimensions of each transmission line. The dimensions of the circuit are 25 mm $\times$ 35 mm.

4.1. Matching Performances

Our goal is to maintain the matching of the circuit despite the change in impedance of the circuit for ensuring robustness in the system. The current flowing through the diode, due to RF-DC conversion

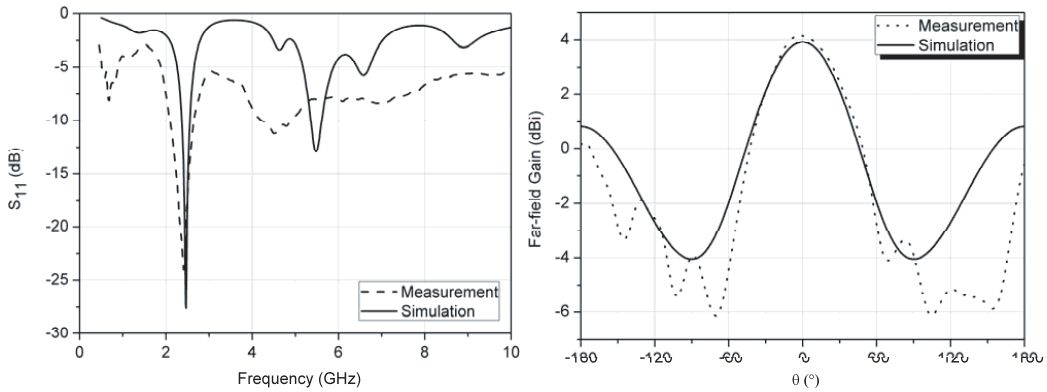

Figure 6. (a) Measured and simulated reflection coefficient of the double monopole antenna, (b) measured and simulated far field realized gain of the double monopole antenna.

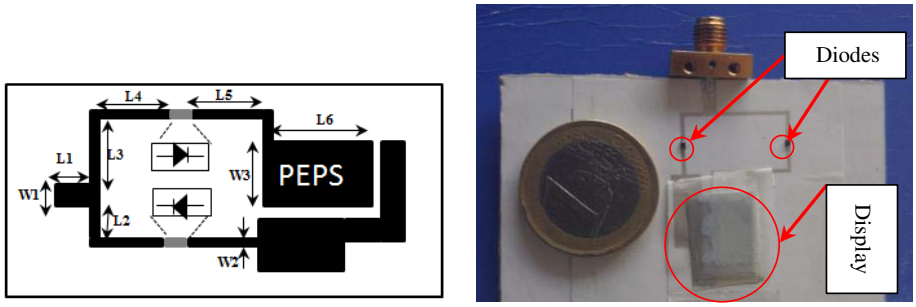

Figure 7. (a) Layout of the rectifier, (b) photograph of the realized rectifier. Dimensions of lines are in mm: $W1 = 2$; $W2 = 0.5$; $W3 = 7$; $L1 = 5$; $L2 = 3.7$; $L3 = 12.8$; $L4 = 5$; $L5 = 5$; $L6 = 15$.

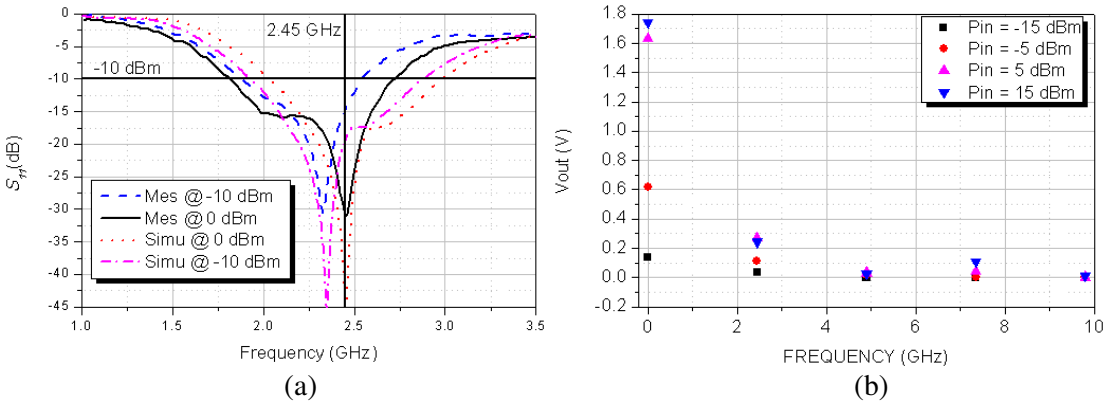

Figure 8. (a) Reflection coefficient variation depending on frequency and incident power, (b) simulated output voltage spectral coefficients.

is not constant. When the power level increases, the diode operates in the nonlinear regime. Then the current through the diode increases being no more negligible compared to saturation current (Is). As a result, the resistance of the diode junction varies, driving a change in the input impedance of circuit [22].

Figure 8(a) describes the variation of the reflection coefficient in function of the frequency for low and high levels of input power. For -10 dBm and 0 dBm, the reflection coefficient is lower than -10 dB

at 2.45 GHz. Moreover, simulations and measurements fit well.

The simulation was performed using "Large Signal S-Parameters" (LSSP) simulator of Advanced Design System (ADS) software since it takes into account the behavior of nonlinear components.

4.2. Output DC Voltage

Figure 8(b) illustrates the highly nonlinear behavior of the rectifier circuit. Output voltage is represented for DC level, fundamental frequency and higher harmonic frequencies for different input power levels. Voltage level increases with input power. At −5 dBm, an output of 600 mV is reached, and 1.6 V can be achieved with 5 dBm. Voltage at high harmonic frequencies is negligible; however, for the fundamental frequency it can reach 0.25 V when DC voltage is equal to 1.7 V. A compromise between input matching and output voltage was chosen in order to be matched at the fundamental frequency and over a large range of input power while ensuring a sufficient output voltage for powering the small devices.

A co-simulation on CST is performed. CST design studio and CST microwave studio simulate simultaneously in order to take into account the model and nonlinear behavior of the diode as well as propagation effects and different kinds of losses.

5. REALIZATION AND MEASUREMENTS RESULTS

Flexography printing method was performed [23]. It is a roll-to-roll technique using only one ink layer. As the "$C4$" paper presents a greater thickness, printing is done on a very thin paper (48 µm) and then pasted on a corrugated paper. The influence of this paper on the circuit performance has been tested by simulation. The influence is negligible. The connector and diodes are fixed with silver paint. The electrochromic display is composed of four layers. Each layer is also printed. Figure 7(b) shows the realized rectifier.

To perform measurements, first, only the rectifier circuit was realized on a corrugated cardboard substrate ($C4$) in order to test its performances and to control the incident power level at the circuit input. The rectifier performance has been measured. By connecting the input port to the signal generator ANRITSU 68367C and the output port to a voltmeter, DC voltage can be measured depending on the power. Figure 10(a) compares measured DC voltage to the simulated one. Measurement fits well with the simulation.

To demonstrate the operation of the entire system, the measurement of the whole rectenna is performed. Figure 9 shows the fabricated rectenna. The rectenna is 45 mm long and 60 mm wide. Figure 9 describes the measurement process. The signal generator ANRITSU 68367C is now connected to a transmitting antenna. It is a dipole antenna having a gain of 4 dBi at 2.45 GHz. It is situated at 17 cm from the rectenna under test. Distance between the two antennas guarantees that it is far-field region ($17\,\text{cm} > 2D^2/\lambda$, where D (antenna width) = 10 cm). The output voltage is measured across the display. Measurement results are described in Figure 10(b). Output voltage is measured depending on power delivered from the signal generator. For an incident power of 5 dBm, the recovered voltage is equal to 200 mV. When measuring the rectifier alone, it recovers 200 mV to −10 dBm. This difference

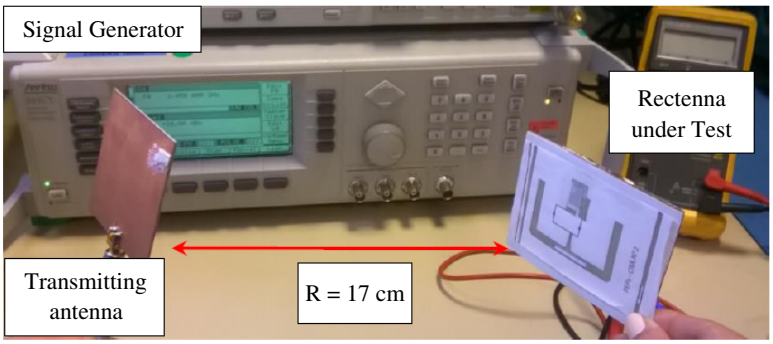

Figure 9. Photograph of measurement process.

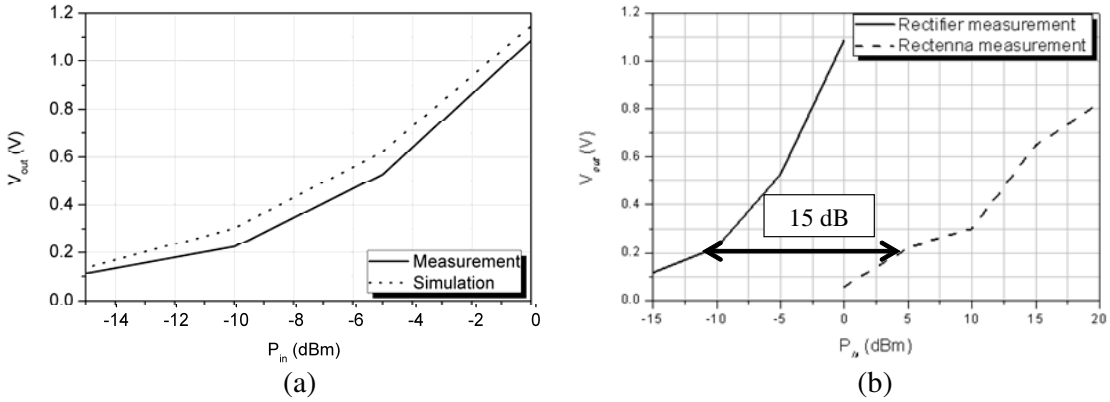

Figure 10. (a) Simulated and measured DC volt age of the rectifier circuit, (b) measured DC voltage of the rectenna.

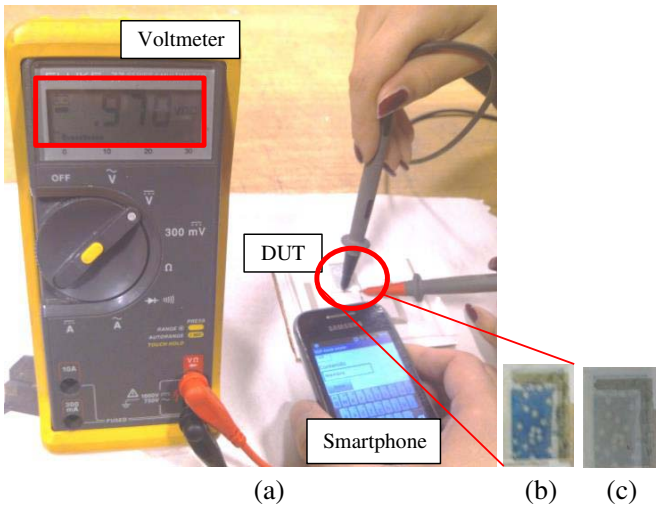

Figure 11. (a) Photograph of measurement process, (b) display on, (c) display off.

of 15 dB has its origin in the propagation losses. Friis Equation (6) is used to calculate the power level at the output of the receiving antenna.

$$P_R = P_T + G_T + G_R + 20 \times \mathrm{Log}\left(\frac{c}{4\pi \times R \times f}\right) \tag{1}$$

where P_R is the power at the input of the rectifier, P_T the power generated by the signal generator, G_T the transmitting antenna gain, G_R the receiving antenna gain and R the distance between the transmitting antenna and the rectenna.

The calculated power from Friis equation is equal to -11.4 dBm. Theoretical and measurement results fit well.

To highlight the application and interest of this circuit concerning the fight against fraud, a smartphone, operating on Wi-Fi mode and configured to send at high-baud rate, is used to send RF power to the receiving antenna. The rectenna, thanks to the two diodes, converts RF power to DC power. To perform the measurement, the device under test is placed in front of the smartphone at a distance of 2 cm and is connected to a voltmeter to measure the output voltage across the display. Figure 11(a) describes the measurement process. Obviously, in that case, the rectenna is placed in a near-field configuration, and the resulting detected power is mainly due to coupling effects between the PiFa antenna of the smartphone and the rectenna. In this configuration, the voltmeter indicates 970 mV. Figures 11(b) and 11(c) present a zoom on the display in "on" and "off" modes to show the contrast between the two states.

6. CONCLUSIONS

This paper describes the optimization process of an EM energy harvesting system. As the circuit was realized on a paper substrate, first investigation step on different paper types has been developed in order to find the most suitable paper type for low-loss, low-consumption electronics. The selected paper is a corrugated cardboard which presents air gaps between its layers. It presents low dielectric losses compared to classical paper substrate, but it is still considered as lossy substrate compared to commercial substrates. The second optimization step consists of making the circuit as compact as possible by using co-design. The resulting rectenna achieved good performances in both near-field and far-field configurations. A voltage of 970 mV is reached when the 60 mm × 45 mm rectenna is placed near a smartphone.

REFERENCES

1. Chang, J., T. Ge, and E. Sanchez-Sinencio, "Challenges of printed electronics on flexible substrates," *Proc. MWSCAS*, 582–585, 2012.
2. Brown, W. C., "The history of power transmission by radio waves," *IEEE Trans. Microwave Theory and Techniques*, Vol. 32, No. 9, 1230–1242, 1984.
3. Sun, H., Y. X. Guo, M. He, and Z. Zhong, "A dual-band rectenna using broadband Yagi antenna array for ambient RF power harvesting," *IEEE Antenna and Wireless Propagation Letters*, Vol. 12, 918–921, 2013.
4. Yamashita, T., K. Honda, and K. Ogawa, "High efficiency MW-band rectenna using a coaxial dielectric resonator and distributed capacitors," *Proc. EMTS*, 823–826, 2013.
5. Zang, F., H. Nam, and J.-C. Lee, "A novel compact folded dipole architecture for 2.45 GHz rectenna application," *Proc. APMC*, 2766–2769, 2009.
6. Alam, S. B., M.-S. Ullah, and S. Moury, "Design of a low power 2.45 GHz RF energy harvesting circuit for rectenna," *Proc. ICIEV*, 1–4, 2013.
7. Tudose, D. S. and A. Voinescu, "Rectifier antenna design for wireless sensor networks," *Proc. CSCS*, 184–188, 2013.
8. Visser, H. J., "Printed folded dipole antenna design for rectenna and RFID application," *Proc. EUCAP*, 2852–2855, 2013.
9. Yang, X. X., C. Jiang, A. Z. Elsherbeni, F. Yang, and Y. Q. Wang, "A novel compact printed rectenna for data communication systems," *IEEE Trans. Antennas and Propagation*, Vol. 61, No. 5, 2532–2539, 2013.
10. Ushiijima, Y., T. Sakamoto, E. Nishiyama, et al., "5.8-GHz integrated differential rectenna unit using both-sided MIC technology with design flexibility," *IEEE Trans. Antennas and Propagation*, Vol. 61, No. 6, 3357–3360, 2013.
11. Adami, S. E., V. Marian, N. Degrenne, et al., "Self-powered ultra-low power DC-DC converter for RF energy harvesting," *Faible Tension Faible Consommation (FTFC), IEEE*, 1–4, 2012.
12. Danine, A., L. Cojocaru, C. Faure, et al., "Room temperature UV treated WO3 thin films for electrochromic devices on paper substrate," *Electrochimica Acta*, Vol. 129, 113–119, 2014.
13. Monk, P. M. S., R. J. Mortimer, and D. R. Rosseinsky, "Electrochromism and electrochromic devices," ISBN-13 978-0-521-82269-5, 2007.
14. Rida, A., L. Yang, R. Vyas, and M. M. Tentzeris, "Conductive inkjet-printed antennas on flexible low-cost paper-based substrates for RFID and WSN applications," *IEEE Antennas and Propagation Magazine*, Vol. 51, No. 3, 13–23, 2009.
15. Kawabata, H., T. Kobayashi, Y. Kobayashi, and Z. Ma, "Measurement accuracy of a TM_{0m0} mode cavity method to measure complex permittivity of rod samples," *Proc. APMC*, 1465–1470, 2006.
16. Ghiotto, A., "Conception d'antennes de tags RFID UHF, application à la réalisation par Jet de matière'," Phd thesis, Institut Polytechnique de Grenoble, 2008.
17. Notingher, P. V., L. Badicu, L. M. Dumitran, et al., "Dielectric losses in cellulose-based insulations," *Proc. SIELMEN*, 169–174, 2009.

18. McSpadden, J., L. Fan, and K. Chang, "Design and experiments of a high-conversion-efficiency 5.8-GHz rectenna," *IEEE Trans. Microwave Theory and Techniques*, Vol. 46, No. 12, 2053–2060, 1998.
19. Takhedmit, H., L. Cirio, Z. Saddi, J.-D. Lan Sun Luk, and O. Picon, "A novel dual-frequency rectifier based on a 180° hybrid junction for RF energy harvesting," *Proc. EUCAP*, 2472–2475, 2013.
20. SKYWORKS, "SMS7630-093: 0201 surface mount silicon Schottky zero bias detector diode," 2008.
21. Franciscatto, B. R., V. Freitas, J.-M. Duchamp, C. Defay, and T. P. Vuong, "A different approach to a highly efficient wireless energy harvesting device for low-power application," *Microwave & Optoelectronics Conference (IMOC), 2013 SBMO/IEEE MTT-S International*, 1–5, 2013.
22. Agilent Technologies, "Diode detector simulation using Agilent technologies EEsof ADS software," Application note 1156.
23. Kharrat, I., G. Eymin Petot Tourtollet, and J. M. Duchamp, et al., "Design and realization of printed on paper antennas," *7th European Conference on Antennas and Propagation*, 3199–3202, Sweden, April 2013.